VNU Journal of Science: Mathematics - Physics

Journal homepage: https://js.vnu.edu.vn/MaP

Original Article

Design and Characteristics of Contactless Small-magnetic-metal Detector Base on Tunnel Magnetoresistance Sensors in Differential Circuit

Pham Van Thanh[1,*], Truong Thi Ngoc Lien[2], Luyen Van Nam[2]

[1]*VNU University of Science, 334 Nguyen Trai, Thanh Xuan, Hanoi, Vietnam*

[2]*IT-BT Convergence Technology Division, Vietnam – Korea Institute of Science and Technology, Hoa lac High-tech Park, km 29 Thang Long Boulevard, Hanoi, Vietnam*

Received 8 December 2023
Revised 22 January 2024; Accepted 16 April 2024

Abstract: Unexpected metal pieces are significant problems for food and pharmaceutical manufacturers. Commonly, conventional coil metal detectors are used to detect these metal pieces. However, these detectors can only detect cm-size metal pieces, making it challenging to detect mm-size metal pieces. This work presents an advanced contactless small-magnetic-metal detector based on tunnel magnetoresistance sensors (TMR). To improve the system's sensitivity, the differential circuit combined with a simple AC-bias lock-in amplifier was designed to reduce the noise of TMR sensors. The sensitivity of this designed detection system is of 0.44 V/mm with a good linearity of R^2=0.82674. The experimental results demonstrate that the fabricated prototype sensors can detect metal wires with a size of 100 μm in diameter and 1 mm in length. Due to a high sensitivity and a low-cost of fabrication, this system is promising to apply on the manufacturing lines for detecting unexpected tiny metal pieces.

Keywords: Tunnel magnetoresistance sensor (TMR), differential circuit, lock-in amplifier, metal detector, magnetic sensor.

1. Introduction

Recently, magnetic field sensors have applications in various fields, such as position tracking, navigation, detection of ferromagnetic objects, guided surgery, space research, nondestructive testing,

* Corresponding author.
E-mail address: phamvanthanh@hus.edu.vn

https//doi.org/10.25073/2588-1124/vnumap.4909

metal detection, etc. [1-4]. There are many candidates for magnetic sensors, such as giant magneto impedance (GMI) sensors [5], anisotropic magnetoresistance (AMR) [6], giant magnetoresistance (GMR) sensors [7], and tunneling magnetoresistance (TMR) sensors [3, 8]. In these candidates, the TMR sensors have been shown to be one of the best sensors for contributions to life and technology because of several advantages, including low cost, high magnetoresistance value, and high sensitivity [9, 10]. Tsukada et al., reported the application of the TMR sensor to detect cracks in steel structures [3]. The TMR sensors were used to measure the concentration of magnetic nanoparticles on the lateral flow strip [11]. Mao et al. used a TMR sensor array to fabricate the advanced metal detector system, which can detect the iron sphere balls with a diameter of 1 mm [8]. The TMR sensor also used to small current effectively proposed by Lei et al., [12]. Furthermore, by using the AC-bias polarity technique combined with the lock-in amplifier and the in differential circuit, the sensitivity and the resolution of the TMR sensor were significantly improved [11, 13]. These studies indicated that the TMR sensor combined with the AC-bias polarity and the differential circuit is a good candidate for use in detecting small metal lines.

In this work, a contactless small-magnetic-metal detector was proposed. The TMR sensors combined with the AC-bias technique and the differential circuit were used to improve the sensitivity of the detector. The iron wires with 100 μm diameter and lengths ranging from 1 to 5 mm were used as samples. The detailed theory, design, experiments, and sensitivity of the proposed detector are presented and discussed.

2. Theory and Methods

2.1. Noise in the Output Signal of the Tmr Sensors

There are various sources of noise in the TMR sensors. Because the TMR sensor is a resistive sensor, it is affected by all kinds of resistive noises, such as shot noise, thermal noise, low-frequency noise, etc. [10]. Specially to measure the DC or low-frequency signals, which are less than 100 Hz [13], the low-frequency noise is dominant and increased inversely with frequency named 1/f noise for most of the magnetic resistive sensors. Therefore, the 1/f noise of TMR is very important and can be expressed by:

$$V_{1/f}(\omega) = \frac{\alpha}{A}\frac{V^2}{f} \tag{1}$$

where α is the 1/f Hooge parameter related to the dimension of the active surface, A is the effective surface area of TMR, f is the frequency, and V is the biased voltage of the TMR sensor[14].

Notably, an important term in Eq. (1) is the frequency (f). In this equation, the frequency of bias voltage is increased inversely with noise. Luong et al., showed that the noise spectrum approaches the white noise if the frequency is larger than 1 kHz [13]. By using the AC-bias polarity combined with the phase-sensitive detection amplifier, the reduced noises can be expected.

2.2. Simple Lock-in Amplifier Method

The lock-in amplifier, also known as a mixer, is a method to recover the real signal from the noise environment of measurements to improve the precision [8]. The basic schematic diagram of a typical lock-in amplifier (LIA) is shown in Fig. 1 [13]. The demodulated output signal of the mixer is the result of the multiplication of the reference input and the sensor's signal output. Suppose B(t) is the AC bias of the TMR-bridge sensor and which is also the input referenced signal A(t):

$$A(t) = B(t) = A_{\text{signal}} \cos(\omega t) \tag{2}$$

The output of the TMR sensor added by noise (Vn) is present as follows:

$$B_{TMR}(t) = B_{signal} \cos(\omega t + \phi) + V_n \tag{3}$$

In this equation, it is supposed that the noise Vn has an angular frequency ω_n and can be expressed as:

$$V_n(t) = A_{noise} \cos(\omega_n t) \tag{4}$$

The output of the mixer is a function of multiplying two signal of the reference signal and the output of the TMR sensor so that this product will be expressed as the trigonometric relation, as follow:

$$\begin{aligned} M_{mixer} &= A(t) \times B_{TMR}(t) = A_{\text{signal}} \cos(\omega t) \times \left(B_{signal} \cos(\omega t + \phi) + V_n \right) \\ &= \frac{1}{2} A_{signal} B_{signal} \left[\cos(2\omega t + \phi) + \cos(\phi) \right] \\ &+ \frac{1}{2} A_{signal} A_{noise} \left[\cos\left((\omega + \omega_s) t \right) + \cos\left((\omega - \omega_s) t \right) \right] \end{aligned} \tag{5}$$

Equation (5) shows that the M_{mixer} includes the high-frequency components of 2ω, $\omega+\omega_n$ and $\omega-\omega_n$; these high-frequency components will be low-pass filtered because they are higher than ones of the designed cut-off frequency of the Low-pass filter (LPF) part. The main modulated signal is the term with cos(ϕ), which is the phase difference between the reference signal and the TMRs' signal output. The demodulated amplitude of LIA depends on this phase difference. Hence, the output signal of an AC-bias polaritied sensor using LIA can be manipulated by changing the phase ϕ. Therefore, the output of LPF is

$$V_o \propto \frac{1}{2} A_{signal} B_{signal} \cos(\phi) \tag{6}$$

This output is a maximum when the signal of TMR and the coherent reference are in phase [10].

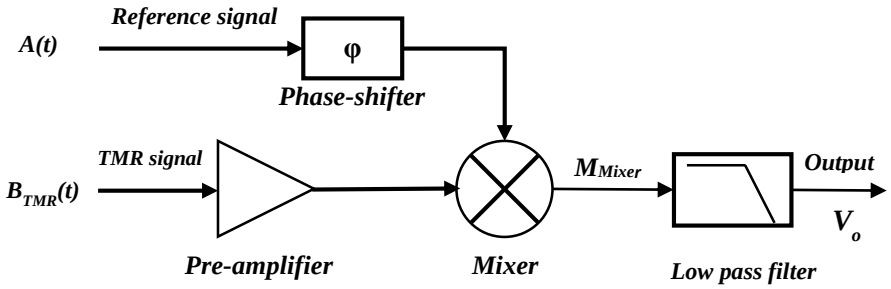

Figure 1. The basic schematic diagram of a typical lock-in amplifier.

2.3. Differential Sensing Method for TMR Sensors

To detect the weak signal of magnetic field H, the differential sensing configuration is proposed by Lei et al., [11]. This configuration is shown in Fig. 2a. Two magnetic sensors, S1 and S2, are the Wheatstone bridge TMR sensors located at 0 and x_0 with a w distance, respectively. An external

magnetic induction $\vec{B}_{ext}$ is perpendicular to the surface of the plastic bar as excitation. The lift-off of sensors is h. The magnetic-metal-wire diameter is significantly smaller than the length.

In this structure, the difference between two TMRs' outputs is expected to improve the signal quality. The two TMRs are in close proximity; therefore, the in-phase noises are canceled due to the differential effects such as the magnetic field of the earth, the magnetic of civil electrical, the magnetic field of near electronic devices, etc. Fig. 2b shows the predicted normalized signal output of each sensor S1 and S2; Fig. 2c shows the differential output of these two signals expressed as [1, 11]

$$H_{x\Delta} = H_{xs2} - H_{xs1} \tag{7}$$

To achieve the best signal, optimizing the distance between two sensors and the lift-off h is essential. In this work, the distance between two sensors (w) is kept at 3mm, and the lift-off (h) is of 2 mm [11].

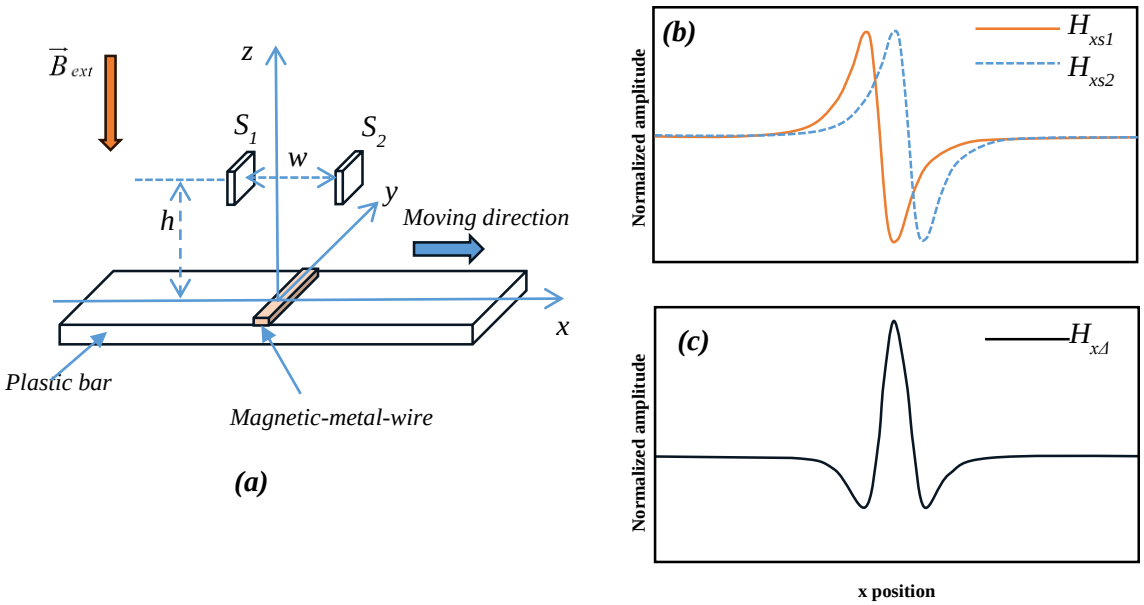

Figure 2. Signals of the differential sensing configuration: (a) measurement diagram, (b) the predicted normalized signal output of each sensor, and (c) the differential signal $H_{x\Delta}$.

3. Circuit Design and Experiment

In this work, TMR2103 sensors from Multidimension Technology Inc. (MDT) were used. This linear sensor utilized a push-pull Wheatstone bridge composed of four unshielded TMR sensor elements. This design provides a high sensitivity differential output, which is linearly proportional to a magnetic field parallel to the sensor's surface. The DFN8L package of TMR2103 was used to design this circuit; therefore, the distance between the centers of sensors is of 3 mm. The sensitivity and noise levels were 6.0 mV/V/Oe and ~10 nT/√Hz@1Hz, respectively. The linear range of TMR2103 was ± 50 Oe, and the saturation range was ± 200 Oe. The AC-bias voltage of TMR2103 sensors was used with 6 Vpp to avoid sensor heating [11]. The frequency of AC-bias voltage is chosen to be 1 kHz to reduce 1/f noise of TMR

sensors [11, 13]. The source of the AC-biased was generated by a function generator FG-7002C (EZ) for both TMR-bridge bias and reference signal of the mixer presented as REF_sig of the designed circuit. The output of TMR2013 was pre-amplified by an instrumentation amplifier (INA128-Texas Instruments) with the advantages of low input bias current, low offset voltage, and high input impedance.

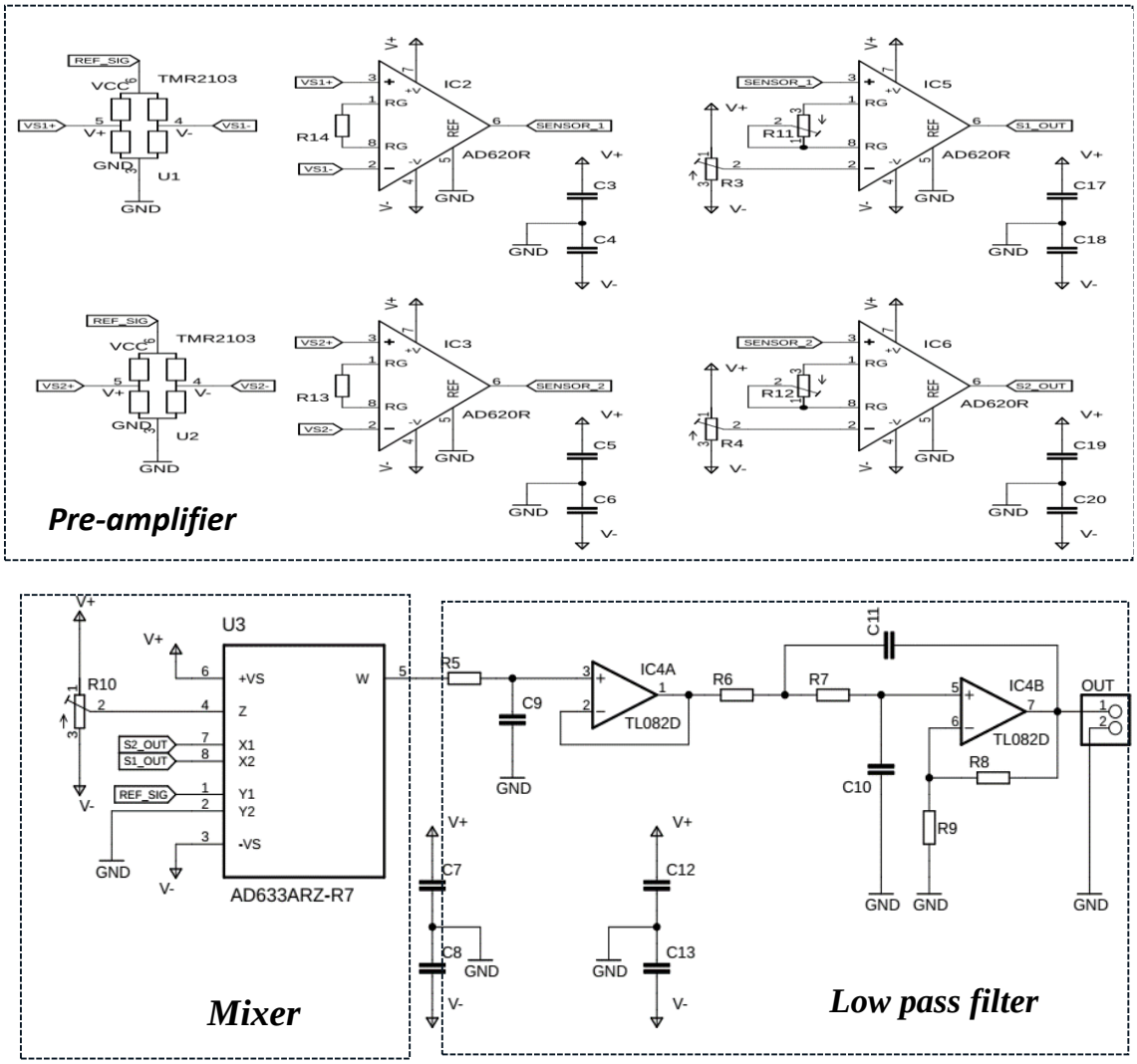

Figure 3. Designed Schematic of an AC-bias differential circuit for TMR2103 sensors.

The gain of the INA128 could be changed by a potentiometer in the circuit and fixed to be ×50 for both pre-amplifiers using R3 and R4 – 10 kΩ potentiometers. The low-cost analog multiplier AD633 chip from Analog Devices is used as the mixer of the designed circuit, which multiplies the reference signal with the pre-amplifier's output signal for TMR2103 sensors. The output of the AD663 is given as follows:

$$M_{mixer} = \frac{A(t) \times B_{TMR}(t)}{10} + Z \tag{8}$$

where $B_{TMR}(t) = S_{2-out} - S_{1-out}$ is the pre-amplified difference signal of two sensors' outputs, A(t) is the reference signal, and Z is the additional DC voltage used to correct the output mixer offset by tuning the R10-10kΩ potentiometer. After that, the demodulated signal is low pass filtered via a second-order active LPF circuit with a cut-off frequency of 5Hz and a fixed gain of ×10 for obtaining the low-frequency signal of mixer output that is proportional to the measured magnetic field. This low-frequency signal is acquired by the Owon SDS1022 oscilloscope. The designed schematic of this detector is shown in Fig. 3.

3. Results and Discussion

The noise performance of the TMR2103 sensor was investigated, the results are shown in Fig. 4. In this measurement, the NI myDAQ combined with LabView was used to measure the 1/f noise spectrum for DC and AC bias with frequency from 1 kHz to 10 kHz. The results showed that noise at 1 Hz is of 88 dB for DC bias, while the noises are of about 95 dB for all frequencies of AC bias from 1 kHz to 10 kHz. The 1/f noise spectrum was approximate to the white noise from the 10 Hz to the higher frequency. These results are consistent with using AC bias for a differential circuit with a frequency of 1 kHz to reduce the 1/f noise mentioned in the circuit design.

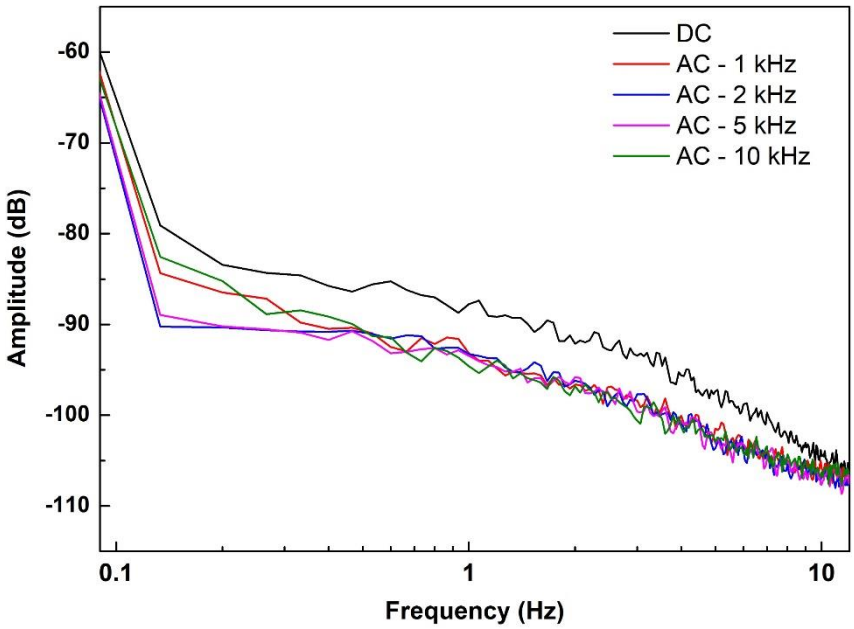

Figure 4. Noise performance of TMR203 sensors with DC and AC bias.

An obtained prototype detector is illustrated in Fig. 5. The two parallel ferrite magnet bars were used to provide a magnetic field perpendicular to the TMR sensors and plastic bar. The dimensions of these magnet bars are of 40 mm, 25 mm, and 10 mm in length, width, and thickness, respectively. The cross-section of 25 × 25 mm^2 and an air gap of 5 mm were designed for C-shaped holder of magnetic bars based on 3D printing. In this experiment, the plastic bar containing a magnetic-metal-wire is moved along the x direction using a linear screw slider controlled by a step motor. The step of the linear screw

slider is of 1 mm. The speed of this motion is fixed at 10 mm/min controlled by Arduino Uno combined with step motor driver DRV 8825.

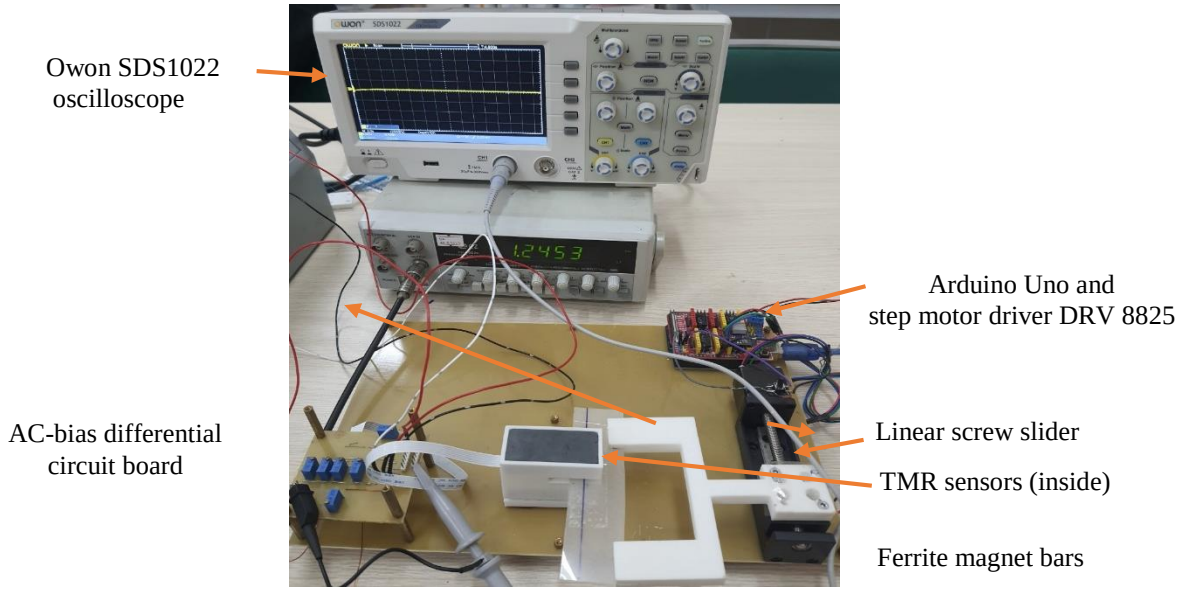

Figure 5. The prototype of designed metal detectors based on tunnel magnetoresistance sensors.

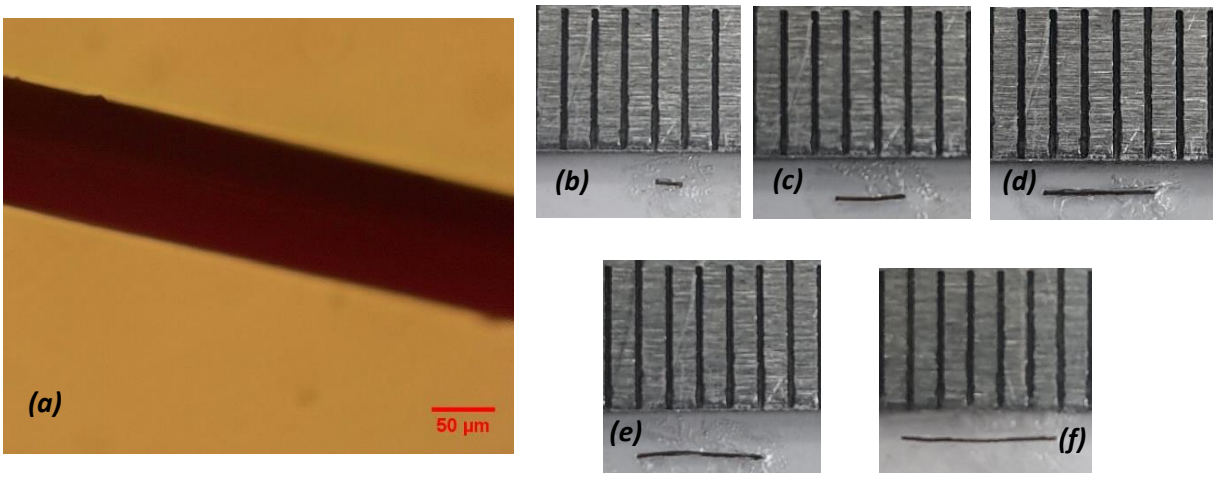

Figure 6. The iron wires for the performance test of the prototype:
(a) photograph of iron wire's diameter;
(b) 1 mm wire; (c) 2 mm wire; (d) 3 mm wire; (e) 4 mm wire; (f) 5 mm wire.

The iron wires with a diameter of 100 µm were used as samples of measurements to evaluate the performance of the detector. These wires' lengths varied from 1mm to 5 mm with a 1 mm step change. The sizes of these iron wires are shown in Fig. 6. The output signals of the prototyped device were shown in Fig. 7a for the five samples of 1, 2, 3, 4, and 5 mm lengths of wire, respectively. The shape of these signals fits well with the theoretical analysis of the differential sensing configuration for TMR sensors. The dependence of the peaks of the output signal on the wire length is shown in Fig. 7b. Based

on the linear fitting of this dependence, the fabricated prototype's sensitivity is estimated to be 0.44 V/mm; the linearity is good with R^2=0.82674. The results indicate that this device has the ability to detect a metal wire as small as 1 mm in length and 100-µm diameter. These results are comparable to the previous researches [1, 3, 8]. Because of its advanced performance, this device can be used to detect the small metal wire with high accuracy.

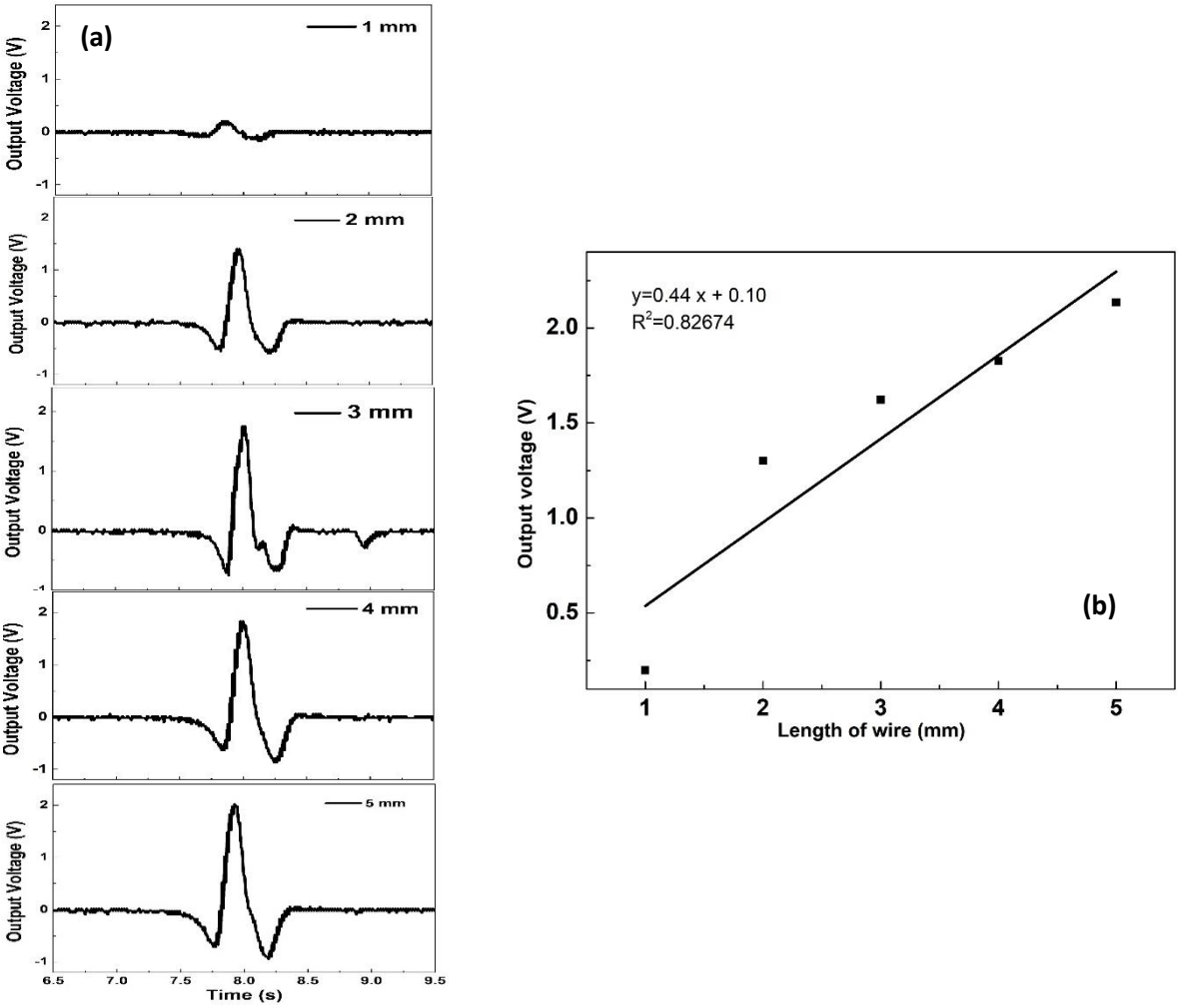

Figure 7. Output signal vs. length of iron wire. (a) Output signal of the prototype system with the length of iron wire changing from 1 mm to 5 mm. (b) Peaks of output signal vs. length of iron wire.

4. Conclusion

In this work, a contactless small-magnetic-metal detector was proposed and fabricated. This detector was designed basing on the TMR2103 sensors combined with AC bias and differential configurations to improve performance. The 1/f noise of TMR2103 was investigated and was consistent with using an AC bias of 1 kHz for a differential circuit to reduce the noise. The output signals of the prototype devices were obtained, fitting well with the theoretical analysis of the differential sensing configuration for TMR

sensors. The experimental results indicated the linear dependence of the peaks of the output signal on the wire length. The sensitivity of this designed detection system is 0.44 V/mm with a good linearity of R^2=0.82674. Notable, this prototype sensor can significantly detect metal wires with a size of 100 μm in diameter and 1 mm in length. Therefore, this device is promising for applications in the detection of small metallic wires with a high accuracy in industrial product lines in the future.

Acknowledgments

This research is funded by the Ministry of Science and Technology (MOST) under grant number of 05.2021M001.

References

[1] H. M. Lei, G. Y. Tian, Broken Wire Detection in Coated Steel Belts Using the Magnetic Flux Leakage Method, Insight: Non-Destructive Testing and Condition Monitoring, Vol. 55, No. 3, 2013, pp. 126-131, https//doi.org/10.1784/insi.2012.55.3.126.

[2] J. E. Davies, J. D. Watts, J. Novotny, D. Huang, P. G. Eames, Magnetoresistive Sensor Detectivity: A Comparative Analysis, 2021, https//doi.org/10.1063/5.0038187.

[3] K. Tsukada, M. Hayashi, Y. Nakamura, K. Sakai, T. Kiwa, Small Eddy Current Testing Sensor Probe Using a Tunneling Magnetoresistance Sensor to Detect Cracks in Steel Structures, IEEE Trans Magn, Vol. 54, No. 11, 2018, https//doi.org/10.1109/TMAG.2018.2845864.

[4] G. P. Conners, Diagnostic uses of Metal Detectors: A Review, [Online]. Available: http://www.scitechantiques.com/belldiscovery/Belltime%20line (accessed on: September 1st, 2023).

[5] L. Zhang, Z. Pan, X. Nie, A Novel Signal Detection Method of Giant Magneto-Impedance Magnetic Sensors, Transactions of the Institute of Measurement and Control, Vol. 35, No. 5, 2012, pp. 625-629, https//doi.org/ 10.1177/0142331212463026.

[6] L. K. Quynh et al., Detection of Magnetic Nanoparticles Using Simple AMR Sensors in Wheatstone Bridge, Journal of Science: Advanced Materials and Devices, Vol. 1, No. 1, 2016, pp. 98-102, https//doi.org/10.1016/j.jsamd.2016.04.006.

[7] C. Marquina et al., GMR Sensors and Magnetic Nanoparticles for Immuno-Chromatographic Assays, J Magn Magn Mater, Vol. 324, No. 21, 2012, pp. 3495-3498, https//doi.org/10.1016/J.JMMM.2012.02.074.

[8] Z. Mao, W. Zhai, Y. Shen, S. Zhao, J. Gao, Advanced Metal Detection System Based on TMR Sensor Array, J Magn Magn Mater, Vol. 543, 2022, https//doi.org/10.1016/j.jmmm.2021.168601.

[9] A. Edelstein, Advances in Magnetometry, Journal of Physics Condensed Matter, Vol. 19, No. 16, 2007, https//doi.org/10.1088/0953-8984/19/16/165217.

[10] Z. Q. Lei, G. J. Li, W. F. Egelhoff, P. T. Lai, P. W. T. Pong, Review of Noise Sources in Magnetic Tunnel Junction Sensors, IEEE Trans Magn, Vol. 47, No. 3, 2011, pp. 602-612, https//doi.org/10.1109/TMAG.2010.2100814.

[11] H. Lei, K. Wang, X. Ji, D. Cui, Contactless Measurement of Magnetic Nanoparticles on Lateral Flow Strips Using Tunneling Magnetoresistance (TMR) Sensors In Differential Configuration, Sensors (Switzerland), Vol. 16, No. 12, 2016, https//doi.org/10.3390/s16122130.

[12] M. Lei et al., Optimal Design and Implementation of Tunnelling Magnetoresistance Based Small Current Sensor with Temperature Compensation, Energy Reports, Vol. 8, 2022, pp. 137-146, https//doi.org/10.1016/j.egyr.2022.08.062.

[13] V. S. Luong, A. T. Nguyen, K. Hoang, Resolution Enhancement in Measuring Low-frequency Magnetic Field of Tunnel Magnetoresistance Sensors with AC-Bias Polarity Technique, Measurement (Lond), Vol. 127, 2018, pp. 512-517, https//doi.org/10.1016/j.measurement.2018.06.027.

[14] F. N. Hooge, 1/f Noise, Physica B+C, Vol. 83, No. 1, 1976, pp. 14-23, https://doi.org/10.1016/0378-4363(76)90089-9.